Measurement of the branching fraction for the decay $\chi_{cJ} \to p\bar{p}\eta\pi^0$

M. Ablikim *et al.*[*]
(BESIII Collaboration)

(Received 18 December 2024; accepted 22 January 2025; published 14 February 2025)

Using $(2712.4 \pm 14.3) \times 10^6 \psi(3686)$ events collected by the BESIII detector operating at the BEPCII collider, we present the first observations of the decays $\chi_{cJ}(J = 0, 1, 2) \to p\bar{p}\eta\pi^0$. Their decay branching fractions are determined to be $\mathcal{B}(\chi_{c0} \to p\bar{p}\eta\pi^0) = (2.42 \pm 0.07 \pm 0.19) \times 10^{-4}$, $\mathcal{B}(\chi_{c1} \to p\bar{p}\eta\pi^0) = (1.95 \pm 0.05 \pm 0.12) \times 10^{-4}$, and $\mathcal{B}(\chi_{c2} \to p\bar{p}\eta\pi^0) = (1.33 \pm 0.05 \pm 0.08) \times 10^{-4}$, where the first uncertainties are statistical and the second systematic.

DOI: 10.1103/PhysRevD.111.032008

I. INTRODUCTION

In the quark model, the $\chi_{cJ}(J = 0, 1, 2)$ mesons are identified as $n^{2S+1}L_J = 1^3P_J$ charmonium states. Due to the principle of parity conservation, their direct production in e^+e^- collisions is suppressed and occurs only through a two-photon exchange process, which results in their low production rates in e^+e^- annihilation. By contrast, the radiative decays of $\psi(3686)$ into χ_{cJ} have branching fractions (BFs) of about 9% [1] and could provide a sizable yield of χ_{cJ} states. The BESIII Collaboration has collected about 2.7 billion $\psi(3686)$ events since 2008 [2], thereby providing an excellent opportunity to investigate the χ_{cJ} properties with the large amounts of the χ_{cJ} mesons produced in the $\psi(3686)$ radiative decays. So far, the sum of all measured BFs of the χ_{cJ} decays are each still far less than 1. Intensive studies of their multibody decays are lacking relative to the few-body decays, particularly for those multibody decays that contains baryon pair. A search for new decay modes is useful in understanding the properties of χ_{cJ}. Furthermore, the χ_{cJ} mesons have different quantum numbers from J/ψ and $\psi(3686)$, so the decays may contain additional information on the potential intermediate baryon and meson states, and also the mass threshold behavior of baryon pair in the multibody system compared to that of the J/ψ and $\psi(3686)$ decays.

In this paper, we investigate the multibody decays $\chi_{cJ} \to p\bar{p}\eta\pi^0$ via the transition process $\psi(3686) \to \gamma\chi_{cJ}$ with $(2712.4 \pm 14.3) \times 10^6 \psi(3686)$ events [2]. Additionally, the potential $p\bar{p}$ threshold enhancement, and the possible intermediate states are searched in the $\eta\pi^0$, $p\eta(\bar{p}\eta)$, and $p\pi^0(\bar{p}\pi^0)$ mass spectrum.

II. BESIII DETECTOR AND MONTE CARLO SIMULATION

The BESIII detector [3] records e^+e^- collisions provided by the BEPCII collider [4]. The cylindrical core of the BESIII detector covers 93% of the full solid angle and consists of a helium-based multilayer drift chamber (MDC), a time-of-flight system (TOF), and a CsI(Tl) electromagnetic calorimeter (EMC), which are all enclosed in a superconducting solenoidal magnet providing a 1.0 T magnetic field. The solenoid is supported by an octagonal flux-return yoke with resistive plate muon identification modules interleaved with steel. The charged-particle momentum resolution at $1\ \mathrm{GeV}/c$ is 0.5%, and the $\mathrm{d}E/\mathrm{d}x$ resolution is 6% for the electrons from Bhabha scattering. The EMC measures photon energies with a resolution of 2.5% (5%) at 1 GeV in the barrel (end cap) region. The time resolution in the plastic scintillator TOF barrel region is 68 ps, while that in the end cap region was 110 ps. The end cap TOF system was upgraded in 2015 using multigap resistive plate chamber technology, providing a time resolution of 60 ps, which benefits ~83% of the data used in this analysis [5–7].

Monte Carlo (MC) simulated data samples produced with a GEANT4-based [8] software package, which includes the geometric description [9] of the BESIII detector and the detector response, are used to determine detection efficiencies and to estimate backgrounds. The simulation models the beam energy spread and initial-state radiation in the e^+e^- annihilation with the generator KKMC [10,11]. The inclusive MC sample includes the production of the $\psi(3686)$ resonance, the ISR production of the J/ψ, and the continuum processes incorporated in KKMC. Particle decays are generated by EVTGEN [12,13] for the known decay modes with BFs taken from the particle data group

[*]Full author list given at the end of the article.

(PDG) [1] and by LUNDCHARM [14,15] for the unknown ones. Final-state radiation from charged final-state particles is included using the PHOTOS package [16].

The signal is simulated with the E1 transition $\psi(3686) \to \gamma\chi_{cJ}$, where the polar angle θ of the radiative photon in the e^+e^- center-of-mass frame is distributed according to $(1 + \lambda\cos^2\theta)$. For $J = 0$, 1, and 2, λ is set to 1, $-\frac{1}{3}$, and $\frac{1}{13}$, respectively [17,18]. The decays $\chi_{cJ} \to p\bar{p}\eta\pi^0$, $\eta \to \gamma\gamma$ and $\pi^0 \to \gamma\gamma$ are generated with the events evenly distributed in the phase space.

III. EVENT SELECTION

In this analysis, both η and π^0 candidates are reconstructed by $\gamma\gamma$ final states. Therefore, the total final state is $5\gamma p\bar{p}$.

Charged tracks detected in the MDC are required to be within a polar angle (θ) range of $|\cos\theta| < 0.93$, where θ is defined with respect to the z-axis, which is the symmetry axis of the MDC. The distance of closest approach to the interaction point (IP) must be less than 10 cm along the z-axis, $|V_z|$, and less than 1 cm in the transverse plane, $|V_{xy}|$. The event candidates must have two good charged tracks with opposite charges. Particle identification (PID) for charged tracks combines measurements of the energy deposited in the MDC (dE/dx) and the flight time in the TOF to form likelihoods $\mathcal{L}(h)(h = p, K, \pi)$ for each hadron h hypothesis. The tracks are identified as protons when the proton hypothesis has the greatest likelihood $[\mathcal{L}(p) > \mathcal{L}(K)$ and $\mathcal{L}(p) > \mathcal{L}(\pi)]$. Finally, the events containing one proton and one antiproton are retained.

Photon candidates are identified using isolated showers in the EMC. The deposited energy of each shower must be greater than 25 MeV in the barrel region ($|\cos\theta| < 0.80$) and more than 50 MeV in the end cap regions ($0.86 < |\cos\theta| < 0.92$). To suppress electronic noise and showers unrelated to the event, the difference between the EMC time and the event start time is required to be within [0, 700] ns. The number of photon candidates is required to be at least five in an event.

In order to suppress backgrounds and improve the mass resolution, a six-constraint (6C) kinematic fit is performed with the $\psi(3686) \to \gamma p\bar{p}\eta\pi^0$ hypothesis by constraining the total four-momentum of the final state particles to that of the colliding beams, and the extra 2C is used to constraint the invariant masses of the photon pairs to the η and π^0 nominal masses [1], respectively. If the 6C kinematic fit converges for more than one combination of the photons, the one with the least χ^2_{6C} is chosen. Furthermore, the selection $\chi^2_{6C} < 20$ is applied, by optimizing a figure of merit defined as $S/\sqrt{S+B}$, where S denotes the number of signal events obtained from the MC simulation that scaled by the following normalized formula, $N^{\rm normalized} = \epsilon_{\chi_{c0}} \cdot N^{\rm Data}_{\psi(3686)} \cdot \mathcal{B}(\psi(3686) \to \gamma\chi_{c0}) \cdot \mathcal{B}(\eta \to \gamma\gamma) \cdot \mathcal{B}(\pi^0 \to \gamma\gamma) \cdot \mathcal{B}(\chi_{c0} \to p\bar{p}\eta\pi^0)$, where the $\chi_{c0} \to \bar{p}p\eta\pi^0$ is the measured branching fraction in this analysis, while B is the number of background events obtained from the inclusive MC sample. Moreover, in order to suppress the backgrounds with four or six photons, a 4C kinematic fit is performed for both signal and background channels by looping all photon combinations according to the different numbers of photons hypothesis. The one with the least χ^2 is kept for each channel. Then, we require

$$\chi^2_{4C}(5\gamma p\bar{p}) < \chi^2_{4C}(4\gamma p\bar{p}), \tag{1}$$

$$\chi^2_{4C}(5\gamma p\bar{p}) < \chi^2_{4C}(6\gamma p\bar{p}). \tag{2}$$

To suppress backgrounds of $\chi_{cJ} \to (\gamma\gamma)p\bar{p}\eta\eta(\pi^0\pi^0)$, we also require

$$\chi^2_{6C}(\gamma p\bar{p}\eta\pi^0) < \chi^2_{6C}(\gamma p\bar{p}\eta\eta), \tag{3}$$

$$\chi^2_{6C}(\gamma p\bar{p}\eta\pi^0) < \chi^2_{6C}(p\bar{p}\eta\eta), \tag{4}$$

$$\chi^2_{6C}(\gamma p\bar{p}\eta\pi^0) < \chi^2_{6C}(\gamma p\bar{p}\pi^0\pi^0), \tag{5}$$

$$\chi^2_{6C}(\gamma p\bar{p}\eta\pi^0) < \chi^2_{6C}(p\bar{p}\pi^0\pi^0), \tag{6}$$

$$\chi^2_{6C}(\gamma p\bar{p}\eta\pi^0) < \chi^2_{6C}(\gamma\gamma p\bar{p}\pi^0\pi^0). \tag{7}$$

After the aforementioned selection criteria, it is found that a large background component comes from the J/ψ-related channel, as shown in Table I. They are suppressed by requiring the η recoil mass (RM) and the invariant mass of $p\bar{p}\eta$ to be outside the J/ψ mass windows. i.e., $RM(\eta) = \sqrt{(E_{\rm CM} - E_\eta)^2 - (P_\eta)^2}$. Here, $E_{\rm CM}$ is center-of-mass energy for $\psi(3686)$, E_η and P_η is the energy and momentum of η and obtained after 4-C kinematic fit. The optimized mass windows are determined to be $|RM_\eta - m_{J/\psi}| > 7.2$ MeV$/c^2$, and $|M_{p\bar{p}\eta} - m_{J/\psi}| > 21.3$ MeV$/c^2$, where $m_{J/\psi}$ is the J/ψ nominal mass [1].

The remaining background from the process $\chi_{cJ} \to p\bar{p}\pi^0\pi^0$ is suppressed by requiring the $M_{\gamma\gamma}$ to be outside the π^0 mass window. We checked the invariant mass spectrum of all $\gamma\gamma$ combinations for the five candidate

TABLE I. J/ψ related background and its possible intermediate state processes.

Mode
$\psi(3686) \to \eta J/\psi$
$\psi(3686) \to \gamma\chi_{cJ}, \chi_{cJ} \to \gamma J/\psi, J/\psi \to p\bar{p}\eta$
$\psi(3686) \to \pi^0\pi^0 J/\psi, J/\psi \to p\bar{p}\eta$

TABLE II. The estimated numbers of the peaking background events, N_2, and their efficiencies.

Mode	Efficiency (%)	N_2
$\chi_{c1} \to \gamma J/\psi, J/\psi \to \eta p\bar{p}$	0.08	53.9 ± 7.0
$\chi_{c2} \to \gamma J/\psi, J/\psi \to \eta p\bar{p}$	0.05	20.1 ± 2.7
$\chi_{c0} \to \pi^0\pi^0 p\bar{p}$	0.01	36 ± 11
$\chi_{c2} \to \pi^0\pi^0 p\bar{p}$	0.01	14.1 ± 4.7
$\chi_{c1} \to \gamma J/\psi, J/\psi \to \omega p\bar{p}$	0.70	51 ± 11
$\chi_{c2} \to \gamma J/\psi, J/\psi \to \omega p\bar{p}$	0.49	19.4 ± 4.2

photons in ranking with their energies and found four of them form the π^0 signals. The requirements, $|M_{\gamma_1^{\pi^0}\gamma_1^{\eta}} - m_{\pi^0}| > 14.1\,\mathrm{MeV}/c^2$, $|M_{\gamma_1^{\pi^0}\gamma_2^{\eta}} - m_{\pi^0}| > 15\,\mathrm{MeV}/c^2$, $|M_{\gamma_1^{\eta}\gamma^E} - m_{\pi^0}| > 21.3\,\mathrm{MeV}/c^2$, and $|M_{\gamma_2^{\eta}\gamma^E} - m_{\pi^0}| > 19.5\mathrm{MeV}/c^2$, are performed to remove the $p\bar{p}\pi^0\pi^0$ backgrounds, where the γ^E represents radiative photon.

The other remaining potential backgrounds are investigated with the inclusive $\psi(3686)$ MC samples, using the event-type analysis tool TopoAna [19]. It is found that there are several main background channels with the contributions larger than 1% as in Table II. The efficiencies are obtained using the large exclusive MC samples, and the normalized numbers of background events are calculated by the following formula, $N^{\mathrm{normalized}} = \epsilon_{bkg} \cdot N^{\mathrm{Data}}_{\psi(3686)} \cdot \mathrm{Br}(bkg)$, where the $\mathrm{Br}(bkg)$ are the BFs of these different background processes in PDG [1]. The contributions of these backgrounds will be taken into account in the fit to extract the signal yields later.

The continuum background is investigated using the data samples collected at center-of-mass energy of 3.65 GeV with an integrated luminosity of 454 pb^{-1} [20]. There are five events passing the selection criteria, so the contribution from the continuum process is neglected.

Figure 1 shows the $M(p\bar{p}\eta\pi^0)$ distribution with the survived events in data, and clear χ_{cJ} signals are seen. The χ_{c0}, χ_{c1}, and χ_{c2} signal regions are defined as [3.38, 3.45], [3.49, 3.53], and [3.54, 3.58] GeV/c^2, respectively.

IV. SIGNAL YIELDS

To determine signal yields, an unbinned maximum likelihood fit is performed on $M(p\bar{p}\eta\pi^0)$ distribution with the accepted candidates in data. The χ_{cJ} signals described as

$$PDF_{\mathrm{signal}} = (E_\gamma^3 \times BW(M) \times f_d(E_\gamma)) \otimes G(m, \sigma). \qquad (8)$$

Here, PDF is probability density function. And $E_\gamma = (m^2_{\psi(3686)} - m^2)/2m_{\psi(3686)}$ is the energy of the E1 transition photon, where $m_{\psi(3686)}$ is the $\psi(3686)$ nominal mass [1]. $BW(M) = 1/((M - m_{\chi_{cJ}})^2 + 0.25\Gamma^2_{\chi_{cJ}})$ is the Breit-Wigner function, where $m_{\chi_{cJ}}$ and $\Gamma_{\chi_{cJ}}$ are the χ_{cJ} mass and width, respectively, and fixed to the values in the PDG [1]. The function $f_d(E_\gamma)$ is used to damp the diverging tail caused by the E_γ^3 term and is given by $(E_0^2/(E_\gamma E_0 + (E_\gamma - E_0)^2))$, as introduced by the KEDR experiment [21], where $E_0 = (m^2_{\psi(3686)} - m^2_{\chi_{cJ}})/2m_{\psi(3686)}$ denotes the peaking energy of the transition photon. $G(m, \sigma)$ is a Gaussian function accounting for the difference in detector resolution between data and MC simulation, where m denotes the mean and σ denotes standard deviation. These two parameters are free for all χ_{cJ} signals fitting. The smooth background is described with a second-order Chebychev polynomial. The χ_{cJ}-related backgrounds are described by the MC-simulated shapes, and the number of background events are fixed to the values listed in Table II. Figure 1 shows the fitting result. The fit goodness is calculated to be $\chi^2/n.d.f. = 145.7/138$. The obtained signal yields are summarized in Table III.

The potential intermediate states are investigated in the $p\bar{p}$, $\eta\pi^0$, $p\eta/\bar{p}\eta$ and $p\pi^0/\bar{p}\pi^0$ invariant mass spectra as shown in Figs. 2–4. The hints of the scalar meson $a_0(980)$

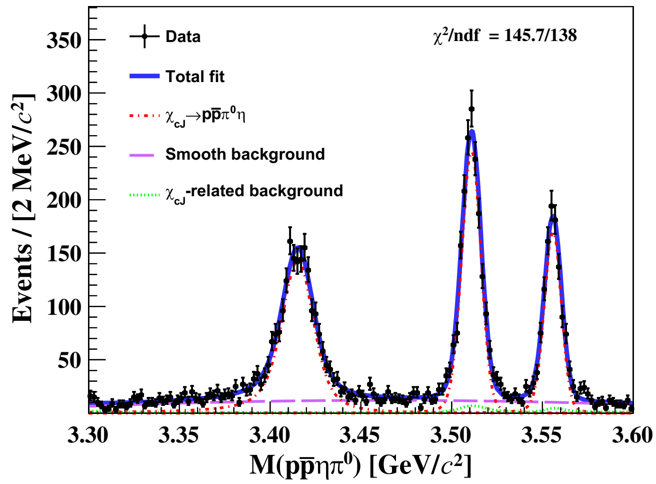

FIG. 1. The fit to the $M(p\bar{p}\eta\pi^0)$ distribution from data, where the points with error bars denote the data, the blue line denote the total fit, the red dashed line denote the signal shape, the purple line denote the smooth background, and the green dashed line denote the χ_{cJ}-related background.

TABLE III. The signal yields $N^{\mathrm{obs}}_{\chi_{cJ}}$, detection efficiencies, and $\mathcal{B}(\chi_{cJ} \to p\bar{p}\eta\pi^0)$, where the first uncertainties are statistical and the second systematic.

$N^{\mathrm{obs}}_{\chi_{cJ}}$		$\epsilon(\chi_{cJ} \to p\bar{p}\eta\pi^0)$ (%)	$\mathcal{B}(\chi_{cJ} \to p\bar{p}\eta\pi^0)$ ($\times 10^{-4}$)
χ_{c0}	1897.8 ± 55.7	7.62 ± 0.2	$2.42 \pm 0.07 \pm 0.19$
χ_{c1}	1694.6 ± 46.7	8.44 ± 0.2	$1.95 \pm 0.05 \pm 0.12$
χ_{c2}	1058.9 ± 37.2	8.04 ± 0.2	$1.33 \pm 0.05 \pm 0.08$

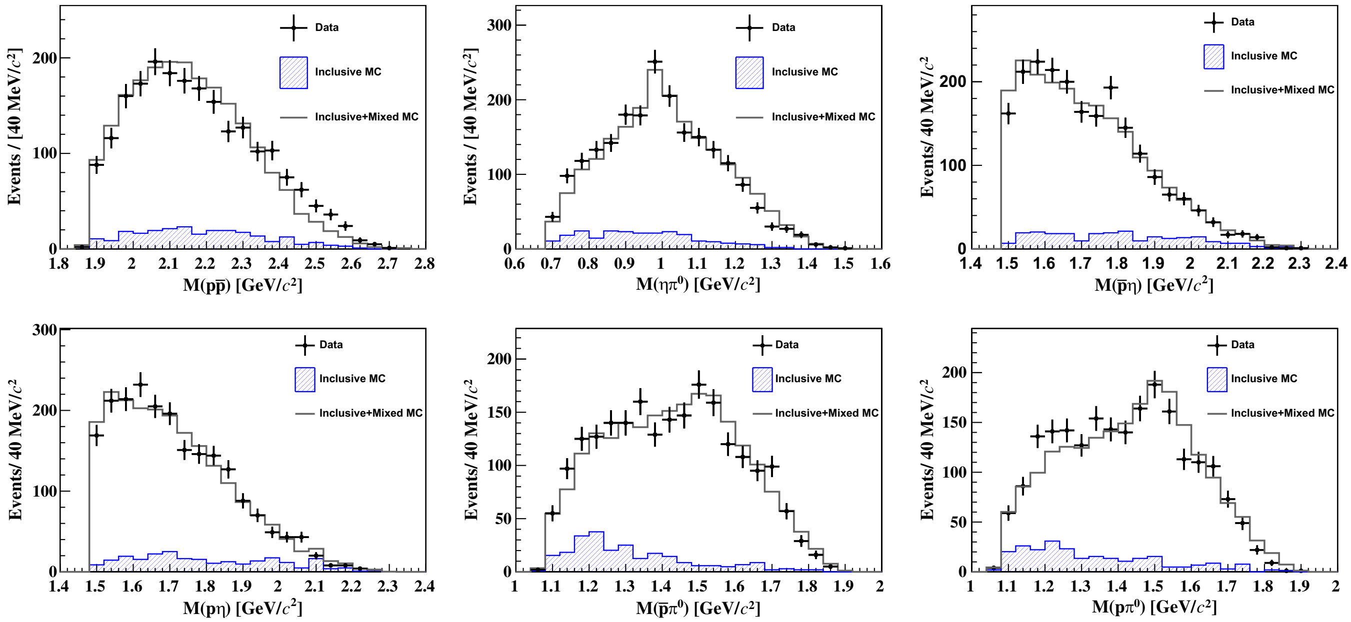

FIG. 2. Comparisons of the distributions of the invariant masses of two-body combinations of the accepted candidates for $\chi_{c0} \to p\bar{p}\eta\pi^0$. The points with error bars denote the data, the shaded histograms denote the background from inclusive MC sample, and the histograms denote the mixed MC sample plus the background contribution.

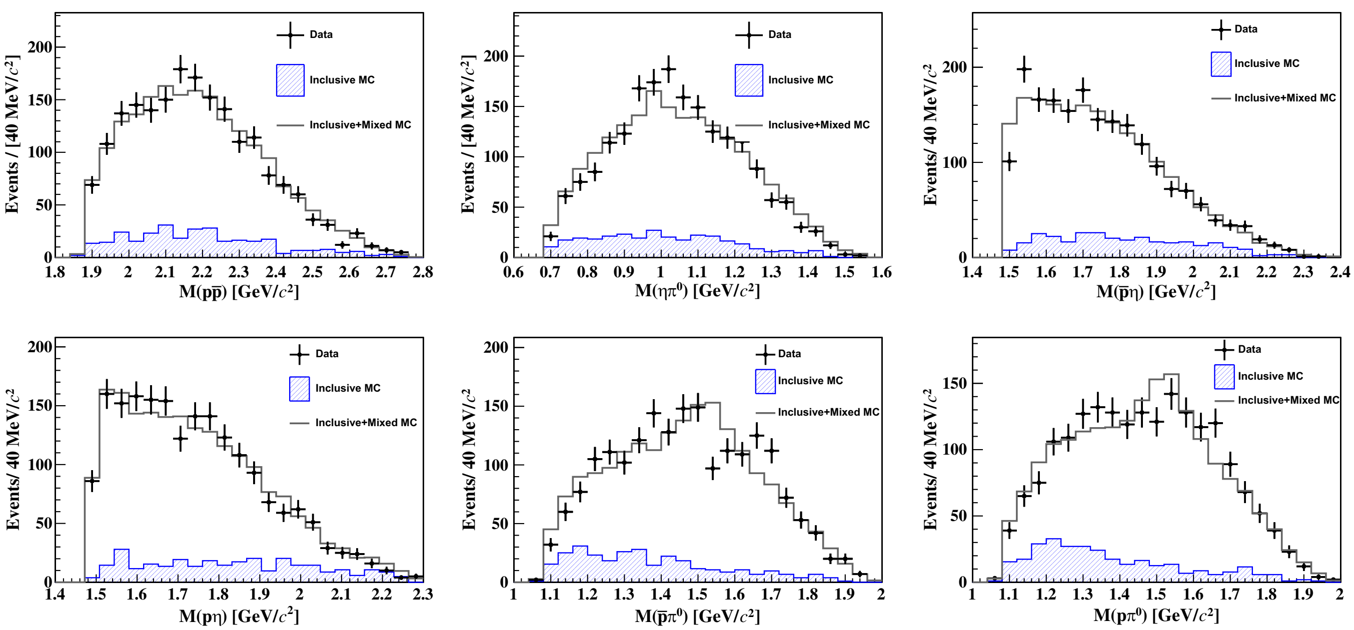

FIG. 3. Comparisons of the distributions of the invariant masses of two-body combinations of the accepted candidates for $\chi_{c1} \to p\bar{p}\eta\pi^0$. The points with error bars denote the data, the shaded histograms denote the background from inclusive MC sample, and the histograms denote the mixed MC sample plus the background contribution.

and the excited baryon $N(1535)$ can be seen. But no significant $p\bar{p}$ threshold enhancement is observed. The numbers of $a_0(980)$ and $N(1535)$ are obtained via one or two-dimensional mass spectrum fits, respectively. The one-dimensional fit to M($\eta\pi^0$) is performed to determine the proportions of $a_0(980)$, while the two-dimensional fits to M($p\pi^0$) vs M($\bar{p}\eta$) and M($\bar{p}\pi^0$) vs M($p\eta$) are performed to determine the proportions of N(1535). Here, the proportions of $\chi_{cJ} \to p\bar{p}a_0(980)$ are approximately 10%, 10% and 10% in the χ_{cJ} signal regions, the proportions of $\chi_{cJ} \to N(1535)\bar{p}\pi^0 + \mathrm{c.c.}$ are approximately 30%, 30% and 30% and $\chi_{cJ} \to N(1535)\bar{p}\eta + \mathrm{c.c.}$ are approximately 30%, 40% and 30%. These fractions are used to generated the mixed MC.

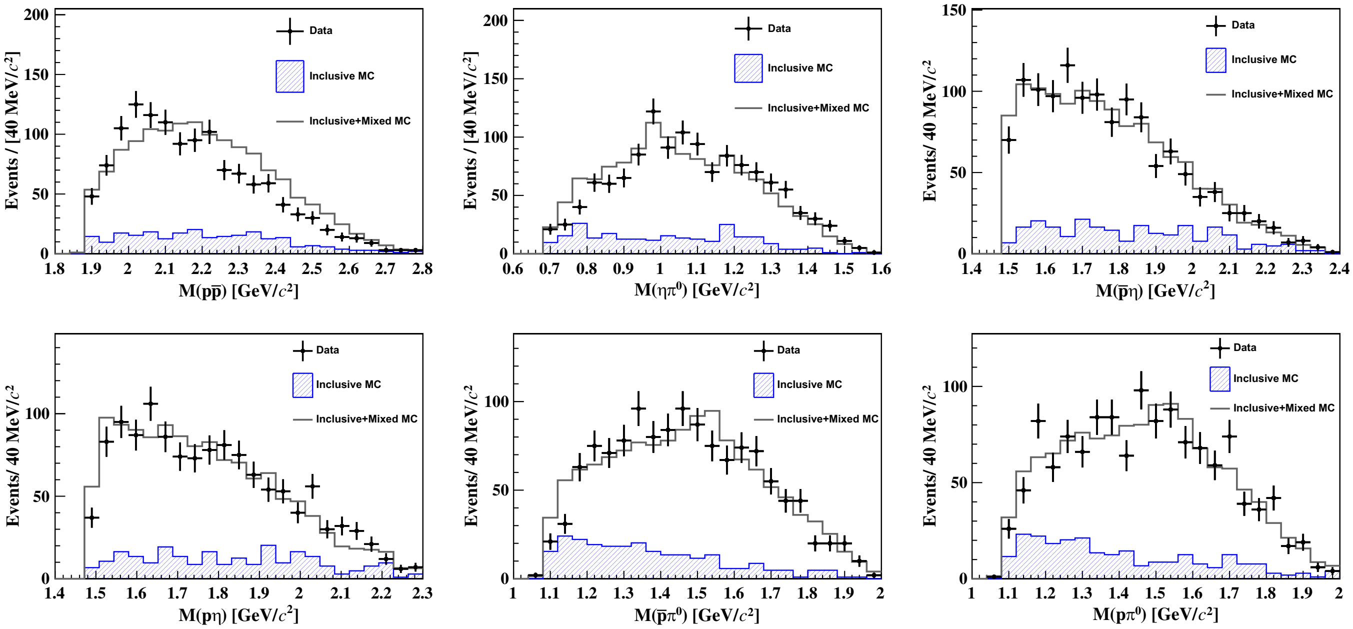

FIG. 4. Comparisons of the distributions of the invariant masses of two-body combinations of the accepted candidates for $\chi_{c2} \to p\bar{p}\eta\pi^0$. The points with error bars denote the data, the shaded histograms denote the background from inclusive MC sample, and the histograms denote the mixed MC sample plus the background contribution.

The BFs of $\chi_{cJ}(J = 0, 1, 2) \to p\bar{p}\eta\pi^0$ are calculated as

$$\mathcal{B}(\chi_{cJ} \to p\bar{p}\eta\pi^0) = \frac{N^{\text{obs}}_{\chi_{cJ}}}{N_{\psi(3686)} \cdot \mathcal{B} \cdot \varepsilon}, \tag{9}$$

where $N^{\text{obs}}_{\chi_{cJ}}$ is the signal yield of $\chi_{cJ} \to p\bar{p}\eta\pi^0$, $N_{\psi(3686)}$ is the number of $\psi(3686)$ events, $\mathcal{B} = \mathcal{B}(\psi(3686) \to \gamma\chi_{cJ}) \cdot \mathcal{B}(\eta \to \gamma\gamma) \cdot \mathcal{B}(\pi^0 \to \gamma\gamma)$, and ε denotes the detection efficiencies obtained from the mixed signal MC samples. The measured BFs are summarized in Table III.

V. SYSTEMATIC UNCERTAINTIES

The systematic uncertainties in the BF measurements originate from several sources, as summarized in Table IV. They are introduced below.

(I) *Tracking:* The uncertainty of the $p\bar{p}$ tracking is estimated by the control sample $J/\psi \to p\bar{p}\pi^+\pi^-$ and is assigned as 1.0% for each $p/\bar{p}$ [22].

(II) *PID:* The uncertainty of the PID of $p\bar{p}$ is studied using the control sample $e^+e^- \to p\bar{p}\pi^0$ and is estimated to be 1.0% for each $p/\bar{p}$ [23].

(III) *Photon selection:* The uncertainty of the photon selection is studied using the control sample $e^+e^- \to \gamma\mu^+\mu^-$ [24] and is determined to be 0.5% for each photon.

(IV) *η and π^0 reconstruction:* The uncertainty from the η and π^0 reconstruction is 1.0% per η or π^0, studied with the high purity control samples $J/\psi \to p\bar{p}\eta$ and $J/\psi \to \pi^+\pi^-\pi^0$ [25].

(V) *Kinematic fit*: The systematic uncertainty of kinematic fit is estimated by comparing the efficiencies with and without applying the helix correction [26]. The correction factors for protons are obtained by studying the control sample $\psi(3686) \to p\bar{p}\pi^0$. The systematic uncertainties are estimated to be 1.9%,

TABLE IV. Relative systematic uncertainties in the measurements of the BFs of $\chi_{cJ} \to p\bar{p}\eta\pi^0$, where the "/" means negligible.

Source	$\chi_{c0}(\%)$	$\chi_{c1}(\%)$	$\chi_{c2}(\%)$
Tracking	2.0	2.0	2.0
PID	2.0	2.0	2.0
Photon	2.5	2.5	2.5
η reconstruction	1.0	1.0	1.0
π^0 reconstruction	1.0	1.0	1.0
Kinematic fit	1.9	2.0	1.9
π^0 mass window	/	/	/
$RM(\eta)$ veto region	0.6	/	/
$M(p\bar{p}\eta)$ veto region	1.0	0.5	0.4
Fitting range	1.3	3.0	2.7
Signal shape	0.1	0.3	1.2
Nonpeaking background	3.5	0.9	0.2
Peaking background	3.4	1.4	0.3
Quoted BFs	2.1	2.5	2.2
MC statistics	0.2	0.2	0.2
MC model	2.7	1.1	0.5
Intermediate states	0.8	0.4	0.1
$N_{\psi(3686)}$	0.5	0.5	0.5
Total	7.7	6.3	5.8

2.0%, and 1.9% for $\chi_{cJ}(J=0,1,2)\to p\bar{p}\eta\pi^0$, respectively.

(VI) *Signal yield*

(i) *Mass window*: We set π^0 and J/ψ mass windows to veto those related backgrounds as mentioned before. To estimate the systematic uncertainties caused by these requirements, we examine the branching fractions by adjusting the relevant mass window. For each background veto, we vary the corresponding mass windows nine times with a step of 0.2 or 0.5 MeV/c^2. Here, 0.2 MeV/c^2 corresponds to the J/ψ recoil mass window, while 0.5 MeV/c^2 corresponds to the J/ψ mass window in $M(p\bar{p}\eta)$) and π^0 mass windows. For each case, the deviation between the alternative and nominal one is defined as $\zeta=\frac{|\mathcal{B}_{\rm nominal}-\mathcal{B}_{\rm test}|}{\sqrt{|\sigma^2_{\mathcal{B},\rm nominal}-\sigma^2_{\mathcal{B},\rm test}|}}$, where $\mathcal{B}$ denotes branching fractions of $\chi_{cJ}\to p\bar{p}\eta\pi^0$ and σ denotes statistical uncertainty. If ζ is less than 2.0, the associated systematic uncertainty is negligible according to the Barlow test [27]. Otherwise, its relative difference is assigned as the systematic uncertainty.

(ii) *Fit method:* The systematic uncertainties due to the fit range are examined by varying the nominal fit range from [3.29, 3.60] to [3.31, 3.60] GeV/c^2, with a step of 2 MeV/c^2, and the Barlow test is performed as above. The systematic uncertainties are 1.3%, 3.0% and 2.7% for $\chi_{cJ}(J=0,1,2)\to p\bar{p}\eta\pi^0$, respectively.

The uncertainty caused by the signal shape is estimated by replacing the damping factor with an alternative damping factor used by CLEO [28], $f_d(E_\gamma)=\exp(-E_\gamma^2/8\beta^2)$, is chosen to estimate the uncertainty from the damping function, where β is a free parameter. The difference between the two damping functions is taken as the systematic uncertainty. They are 0.1%, 0.3%, and 1.2% for $\chi_{cJ}(J=0,1,2)\to p\bar{p}\eta\pi^0$, respectively.

The systematic uncertainty caused by peaking background is estimated by varying the number of events by 1 standard deviation, which includes the statistical uncertainty of the MC simulated sample and the uncertainty related to the BF. The largest differences relative to the nominal BF are assigned as the corresponding systematic uncertainty.

The uncertainty due to the nonpeaking background shape is estimated by replacing the second-order Chebychev polynomial with the third-order Chebychev one. The difference relative to the nominal result is taken as the corresponding systematic uncertainty.

(VII) *Quoted BFs*: The uncertainties due to the quoted BFs of the intermediate states are cited from from the PDG [1].

(VIII) *MC statistics*: The uncertainty due to the limited MC statistics is calculated by $\sqrt{\frac{(1-\varepsilon)\varepsilon}{N}}$, where ε is the detection efficiency and N is the total number of MC events. These uncertainties are all 0.2% for three decay final states.

(IX) *MC model*: The systematic uncertainty due to intermediate states is estimated by comparing the nominal detection efficiency with that obtained with the phase space model, and the differences are determined to be 2.7%, 1.1%, and 0.5% for $\chi_{cJ}(J=0,1,2)\to p\bar{p}\eta\pi^0$, respectively, which are taken as the systematic uncertainties.

(X) *Intermediate states*: The systematic uncertainty due to fitting fractions of intermediate states is estimated by varying the fractions. The largest differences relative to the nominal BFs are assigned as the corresponding systematic uncertainty.

(XI) $N_{\psi(3686)}$: The uncertainty from the total number of $\psi(3686)$ events is determined to be 0.5% [2].

All the systematic uncertainties are summarized in Table IV, where the total uncertainties are obtained by adding all of them in quadrature, assuming all contributions are independent.

VI. SUMMARY

In summary, based on $(2712.4\pm14.3)\times10^6\psi(3686)$ events taken by the BESIII detector, the decays $\chi_{cJ}(J=0,1,2)\to p\bar{p}\eta\pi^0$ are observed for the first time. The corresponding BFs are determined to be $\mathcal{B}(\chi_{c0}\to p\bar{p}\eta\pi^0)=(2.42\pm0.07\pm0.19)\times10^{-4}$, $\mathcal{B}(\chi_{c1}\to p\bar{p}\eta\pi^0)=(1.95\pm0.05\pm0.12)\times10^{-4}$, and $\mathcal{B}(\chi_{c2}\to p\bar{p}\eta\pi^0)=(1.33\pm0.05\pm0.08)\times10^{-4}$, respectively. The observation for this new multibody decay that contains baryon pair will be useful in understanding the properties of χ_{cJ}.

ACKNOWLEDGMENTS

The BESIII Collaboration thanks the staff of BEPCII and the IHEP computing center for their strong support. This work is supported in part by National Key R and D Program of China under Contracts No. 2020YFA0406300, No. 2020YFA0406400; National Natural Science Foundation of China (NSFC) under Contracts No. 11635010, No. 11735014, No. 11835012, No. 11935015, No. 11935016, No. 11935018, No. 11961141012, No. 12022510, No. 12025502, No. 12035009, No. 12035013, No. 12061131003, No. 12192260, No. 12192261, No. 12192262, No. 12192263, No. 12192264, No. 12192265, No. 12221005, No. 12225509, No. 12235017, No. 12150004, No. 12475197, No. 12275067, and

No. 11875033; Program of Science and Technology Development Plan of Jilin Province of China under Contracts No. 20210508047RQ and No. 20230101021JC; The Science and Technology R&D Program Joint Fund Project of Henan Province (Grant No. 225200810030) and the Science and Technology Innovation Leading Talent Support Program of Henan Province; the Chinese Academy of Sciences (CAS) Large-Scale Scientific Facility Program; the CAS Center for Excellence in Particle Physics (CCEPP); Joint Large-Scale Scientific Facility Funds of the NSFC and CAS under Contract No. U1832207; CAS Key Research Program of Frontier Sciences under Contracts No. QYZDJ-SSW-SLH003, No. QYZDJ-SSW-SLH040; 100 Talents Program of CAS; The Institute of Nuclear and Particle Physics (INPAC) and Shanghai Key Laboratory for Particle Physics and Cosmology; European Union's Horizon 2020 research and innovation programme under Marie Sklodowska-Curie grant agreement under Contract No. 894790; German Research Foundation DFG under Contracts No. 455635585, Collaborative Research Center CRC 1044, No. FOR5327, No. GRK 2149; Istituto Nazionale di Fisica Nucleare, Italy; Ministry of Development of Turkey under Contract No. DPT2006K-120470; National Research Foundation of Korea under Contract No. NRF-2022R1A2C1092335; National Science and Technology fund of Mongolia; National Science Research and Innovation Fund (NSRF) via the Program Management Unit for Human Resources and Development, Research and Innovation of Thailand under Contract No. B16F640076; Polish National Science Centre under Contract No. 2019/35/O/ST2/02907; The Swedish Research Council; U.S. Department of Energy under Contract No. DE-FG02-05ER41374.

DATA AVAILABILITY

The data that support the findings of this article are not publicly available. The data are available from the authors upon reasonable request.

[1] S. Navas *et al.* (Particle Data Group), Phys. Rev. D **110**, 030001 (2024).
[2] M. Ablikim *et al.* (BESIII Collaboration), Chin. Phys. C **48**, 093001 (2024).
[3] M. Ablikim *et al.* (BESIII Collaboration), Nucl. Instrum. Methods Phys. Res., Sect. A **614**, 345 (2010).
[4] C. H. Yu *et al.*, in *Proceedings of IPAC2016, Busan, Korea* (JACoW, Busan, 2016).
[5] X. Li *et al.*, Radiat. Detect. Technol. Methods **1**, 13 (2017).
[6] Y. X. Guo *et al.*, Radiat. Detect. Technol. Methods **1**, 15 (2017).
[7] P. Cao *et al.*, Nucl. Instrum. Methods Phys. Res., Sect. A **953**, 163053 (2020).
[8] S. Agostinelli *et al.* (GEANT4 Collaboration), Nucl. Instrum. Methods Phys. Res., Sect. A **506**, 250 (2003).
[9] K. X. Huang *et al.*, Nucl. Sci. Tech. **33**, 142 (2022).
[10] S. Jadach, B. F. L. Ward, and Z. Wąs, Comput. Phys. Commun. **130**, 260 (2000).
[11] S. Jadach, B. F. L. Ward, and Z. Wąs, Phys. Rev. D **63**, 113009 (2001).
[12] R. G. Ping, Chin. Phys. C **32**, 599 (2008).
[13] D. J. Lange, Nucl. Instrum. Methods Phys. Res., Sect. A **462**, 152 (2001).
[14] J. C. Chen, G. S. Huang, X. R. Qi, D. H. Zhang, and Y. S. Zhu, Phys. Rev. D **62**, 034003 (2000).
[15] R. L. Yang, R. G. Ping, and H. Chen, Chin. Phys. Lett. **31**, 061301 (2014).
[16] E. Richter-Was, Phys. Lett. B **303**, 163 (1993).
[17] W. Tanenbaum *et al.*, Phys. Rev. D **17**, 1731 (1978).
[18] G. R. Liao, R. G. Ping, and Y. X. Yang, Chin. Phys. Lett. **26**, 051101 (2009).
[19] X. Y. Zhou, S. X. Du, G. Li, and C. P. Shen, Comput. Phys. Commun. **258**, 107540 (2021).
[20] M. Ablikim *et al.* (BESIII Collaboration), Chin. Phys. C **37**, 123001 (2013).
[21] V. V. Anashin *et al.* (KEDR Collaboration), Int. J. Mod. Phys. Conf. Ser. **02**, 188 (2011).
[22] W. L. Yuan, X. C. Ai, X. B. Ji, S. J. Chen, Y. Zhang, L. H. Wu, L. L. Wang, and Y. Yuan, Chin. Phys. C **40**, 026201 (2016).
[23] M. Ablikim *et al.* (BESIII Collaboration), Phys. Rev. D **86**, 092009 (2012).
[24] M. Ablikim *et al.* (BESIII Collaboration), Phys. Rev. D **109**, 032006 (2024).
[25] M. Ablikim *et al.* (BESIII Collaboration), Phys. Rev. D **81**, 052005 (2010).
[26] M. Ablikim *et al.* (BESIII Collaboration), Phys. Rev. D **87**, 012002 (2013).
[27] O. Behnke, K. Kröninger, G. Schott, and T. Schörner-Sadenius, *Data Analysis in High Energy Physics: A Practical Guide to Statistical Methods* (Wiley-VCH, Berlin, Germany, 2013).
[28] R. E. Mitchell *et al.* (CLEO Collaboration), Phys. Rev. Lett. **102**, 011801 (2009).

M. Ablikim,[1] M. N. Achasov,[4,c] P. Adlarson,[76] O. Afedulidis,[3] X. C. Ai,[81] R. Aliberti,[35] A. Amoroso,[75a,75c] Q. An,[72,58,a] Y. Bai,[57] O. Bakina,[36] I. Balossino,[29a] Y. Ban,[46,h] H.-R. Bao,[64] V. Batozskaya,[1,44] K. Begzsuren,[32] N. Berger,[35] M. Berlowski,[44] M. Bertani,[28a] D. Bettoni,[29a] F. Bianchi,[75a,75c] E. Bianco,[75a,75c] A. Bortone,[75a,75c] I. Boyko,[36] R. A. Briere,[5] A. Brueggemann,[69] H. Cai,[77] X. Cai,[1,58] A. Calcaterra,[28a] G. F. Cao,[1,64] N. Cao,[1,64] S. A. Cetin,[62a] X. Y. Chai,[46,h] J. F. Chang,[1,58] G. R. Che,[43] Y. Z. Che,[1,58,64] G. Chelkov,[36,b] C. Chen,[43] C. H. Chen,[9] Chao Chen,[55] G. Chen,[1] H. S. Chen,[1,64] H. Y. Chen,[20] M. L. Chen,[1,58,64] S. J. Chen,[42] S. L. Chen,[45] S. M. Chen,[61] T. Chen,[1,64] X. R. Chen,[31,64] X. T. Chen,[1,64] Y. B. Chen,[1,58] Y. Q. Chen,[34] Z. J. Chen,[25,i] S. K. Choi,[10] G. Cibinetto,[29a] F. Cossio,[75c] J. J. Cui,[50] H. L. Dai,[1,58] J. P. Dai,[79] A. Dbeyssi,[18] R. E. de Boer,[3] D. Dedovich,[36] C. Q. Deng,[73] Z. Y. Deng,[1] A. Denig,[35] I. Denysenko,[36] M. Destefanis,[75a,75c] F. De Mori,[75a,75c] B. Ding,[67,1] X. X. Ding,[46,h] Y. Ding,[34] Y. Ding,[40] J. Dong,[1,58] L. Y. Dong,[1,64] M. Y. Dong,[1,58,64] X. Dong,[77] M. C. Du,[1] S. X. Du,[81] Y. Y. Duan,[55] Z. H. Duan,[42] P. Egorov,[36,b] G. F. Fan,[42] J. J. Fan,[19] Y. H. Fan,[45] J. Fang,[1,58] J. Fang,[59] S. S. Fang,[1,64] W. X. Fang,[1] Y. Q. Fang,[1,58] R. Farinelli,[29a] L. Fava,[75b,75c] F. Feldbauer,[3] G. Felici,[28a] C. Q. Feng,[72,58] J. H. Feng,[59] Y. T. Feng,[72,58] M. Fritsch,[3] C. D. Fu,[1] J. L. Fu,[64] Y. W. Fu,[1,64] H. Gao,[64] X. B. Gao,[41] Y. N. Gao,[19] Y. N. Gao,[46,h] Yang Gao,[72,58] S. Garbolino,[75c] I. Garzia,[29a,29b] P. T. Ge,[19] Z. W. Ge,[42] C. Geng,[59] E. M. Gersabeck,[68] A. Gilman,[70] K. Goetzen,[13] L. Gong,[40] W. X. Gong,[1,58] W. Gradl,[35] S. Gramigna,[29a,29b] M. Greco,[75a,75c] M. H. Gu,[1,58] Y. T. Gu,[15] C. Y. Guan,[1,64] A. Q. Guo,[31,64] L. B. Guo,[41] M. J. Guo,[50] R. P. Guo,[49] Y. P. Guo,[12,g] A. Guskov,[36,b] J. Gutierrez,[27] K. L. Han,[64] T. T. Han,[1] F. Hanisch,[3] X. Q. Hao,[19] F. A. Harris,[66] K. K. He,[55] K. L. He,[1,64] F. H. Heinsius,[3] C. H. Heinz,[35] Y. K. Heng,[1,58,64] C. Herold,[60] T. Holtmann,[3] P. C. Hong,[34] G. Y. Hou,[1,64] X. T. Hou,[1,64] Y. R. Hou,[64] Z. L. Hou,[1] B. Y. Hu,[59] H. M. Hu,[1,64] J. F. Hu,[56,j] Q. P. Hu,[72,58] S. L. Hu,[12,g] T. Hu,[1,58,64] Y. Hu,[1] G. S. Huang,[72,58] K. X. Huang,[59] L. Q. Huang,[31,64] P. Huang,[42] X. T. Huang,[50] Y. P. Huang,[1] Y. S. Huang,[59] T. Hussain,[74] F. Hölzken,[3] N. Hüsken,[35] N. in der Wiesche,[69] J. Jackson,[27] S. Janchiv,[32] Q. Ji,[1] Q. P. Ji,[19] W. Ji,[1,64] X. B. Ji,[1,64] X. L. Ji,[1,58] Y. Y. Ji,[50] X. Q. Jia,[50] Z. K. Jia,[72,58] D. Jiang,[1,64] H. B. Jiang,[77] P. C. Jiang,[46,h] S. S. Jiang,[39] T. J. Jiang,[16] X. S. Jiang,[1,58,64] Y. Jiang,[64] J. B. Jiao,[50] J. K. Jiao,[34] Z. Jiao,[23] S. Jin,[42] Y. Jin,[67] M. Q. Jing,[1,64] X. M. Jing,[64] T. Johansson,[76] S. Kabana,[33] N. Kalantar-Nayestanaki,[65] X. L. Kang,[9] X. S. Kang,[40] M. Kavatsyuk,[65] B. C. Ke,[81] V. Khachatryan,[27] A. Khoukaz,[69] R. Kiuchi,[1] O. B. Kolcu,[62a] B. Kopf,[3] M. Kuessner,[3] X. Kui,[1,64] N. Kumar,[26] A. Kupsc,[44,76] W. Kühn,[37] W. N. Lan,[19] T. T. Lei,[72,58] Z. H. Lei,[72,58] M. Lellmann,[35] T. Lenz,[35] C. Li,[47] C. Li,[43] C. H. Li,[39] Cheng Li,[72,58] D. M. Li,[81] F. Li,[1,58] G. Li,[1] H. B. Li,[1,64] H. J. Li,[19] H. N. Li,[56,j] Hui Li,[43] J. R. Li,[61] J. S. Li,[59] K. Li,[1] K. L. Li,[19] L. J. Li,[1,64] Lei Li,[48] M. H. Li,[43] P. L. Li,[64] P. R. Li,[38,k,l] Q. M. Li,[1,64] Q. X. Li,[50] R. Li,[17,31] T. Li,[50] T. Y. Li,[43] W. D. Li,[1,64] W. G. Li,[1,a] X. Li,[1,64] X. H. Li,[72,58] X. L. Li,[50] X. Y. Li,[1,8] X. Z. Li,[59] Y. Li,[19] Y. G. Li,[46,h] Z. J. Li,[59] Z. Y. Li,[79] C. Liang,[42] H. Liang,[72,58] Y. F. Liang,[54] Y. T. Liang,[31,64] G. R. Liao,[14] Y. P. Liao,[1,64] J. Libby,[26] A. Limphirat,[60] C. C. Lin,[55] C. X. Lin,[64] D. X. Lin,[31,64] T. Lin,[1] B. J. Liu,[1] B. X. Liu,[77] C. Liu,[34] C. X. Liu,[1] F. Liu,[1] F. H. Liu,[53] Feng Liu,[6] G. M. Liu,[56,j] H. Liu,[38,k,l] H. B. Liu,[15] H. H. Liu,[1] H. M. Liu,[1,64] Huihui Liu,[21] J. B. Liu,[72,58] K. Liu,[38,k,l] K. Y. Liu,[40] Ke Liu,[22] L. Liu,[72,58] L. C. Liu,[43] Lu Liu,[43] M. H. Liu,[12,g] P. L. Liu,[1] Q. Liu,[64] S. B. Liu,[72,58] T. Liu,[12,g] W. K. Liu,[43] W. M. Liu,[72,58] X. Liu,[38,k,l] X. Liu,[39] Y. Liu,[38,k,l] Y. Liu,[81] Y. B. Liu,[43] Z. A. Liu,[1,58,64] Z. D. Liu,[9] Z. Q. Liu,[50] X. C. Lou,[1,58,64] F. X. Lu,[59] H. J. Lu,[23] J. G. Lu,[1,58] Y. Lu,[7] Y. P. Lu,[1,58] Z. H. Lu,[1,64] C. L. Luo,[41] J. R. Luo,[59] M. X. Luo,[80] T. Luo,[12,g] X. L. Luo,[1,58] X. R. Lyu,[64] Y. F. Lyu,[43] F. C. Ma,[40] H. Ma,[79] H. L. Ma,[1] J. L. Ma,[1,64] L. L. Ma,[50] L. R. Ma,[67] Q. M. Ma,[1] R. Q. Ma,[1,64] R. Y. Ma,[19] T. Ma,[72,58] X. T. Ma,[1,64] X. Y. Ma,[1,58] Y. M. Ma,[31] F. E. Maas,[18] I. MacKay,[70] M. Maggiora,[75a,75c] S. Malde,[70] Y. J. Mao,[46,h] Z. P. Mao,[1] S. Marcello,[75a,75c] Y. H. Meng,[64] Z. X. Meng,[67] J. G. Messchendorp,[13,65] G. Mezzadri,[29a] H. Miao,[1,64] T. J. Min,[42] R. E. Mitchell,[27] X. H. Mo,[1,58,64] B. Moses,[27] N. Yu. Muchnoi,[4,c] J. Muskalla,[35] Y. Nefedov,[36] F. Nerling,[18,e] L. S. Nie,[20] I. B. Nikolaev,[4,c] Z. Ning,[1,58] S. Nisar,[11,m] Q. L. Niu,[38,k,l] W. D. Niu,[55] Y. Niu,[50] S. L. Olsen,[10,64] Q. Ouyang,[1,58,64] S. Pacetti,[28b,28c] X. Pan,[55] Y. Pan,[57] A. Pathak,[10] Y. P. Pei,[72,58] M. Pelizaeus,[3] H. P. Peng,[72,58] Y. Y. Peng,[38,k,l] K. Peters,[13,e] J. L. Ping,[41] R. G. Ping,[1,64] S. Plura,[35] V. Prasad,[33] F. Z. Qi,[1] H. R. Qi,[61] M. Qi,[42] S. Qian,[1,58] W. B. Qian,[64] C. F. Qiao,[64] J. H. Qiao,[19] J. J. Qin,[73] L. Q. Qin,[14] L. Y. Qin,[72,58] X. P. Qin,[12,g] X. S. Qin,[50] Z. H. Qin,[1,58] J. F. Qiu,[1] Z. H. Qu,[73] C. F. Redmer,[35] K. J. Ren,[39] A. Rivetti,[75c] M. Rolo,[75c] G. Rong,[1,64] Ch. Rosner,[18] M. Q. Ruan,[1,58] S. N. Ruan,[43] N. Salone,[44] A. Sarantsev,[36,d] Y. Schelhaas,[35] K. Schoenning,[76] M. Scodeggio,[29a] K. Y. Shan,[12,g] W. Shan,[24] X. Y. Shan,[72,58] Z. J. Shang,[38,k,l] J. F. Shangguan,[16] L. G. Shao,[1,64] M. Shao,[72,58] C. P. Shen,[12,g] H. F. Shen,[1,8] W. H. Shen,[64] X. Y. Shen,[1,64] B. A. Shi,[64] H. Shi,[72,58] J. L. Shi,[12,g] J. Y. Shi,[1] S. Y. Shi,[73] X. Shi,[1,58] J. J. Song,[19] T. Z. Song,[59] W. M. Song,[34,1] Y. J. Song,[12,g] Y. X. Song,[46,h,n] S. Sosio,[75a,75c] S. Spataro,[75a,75c] F. Stieler,[35] S. S. Su,[40] Y. J. Su,[64] G. B. Sun,[77] G. X. Sun,[1] H. Sun,[64] H. K. Sun,[1] J. F. Sun,[19] K. Sun,[61] L. Sun,[77] S. S. Sun,[1,64] T. Sun,[51,f] Y. J. Sun,[72,58] Y. Z. Sun,[1] Z. Q. Sun,[1,64] Z. T. Sun,[50] C. J. Tang,[54] G. Y. Tang,[1] J. Tang,[59] M. Tang,[72,58] Y. A. Tang,[77] L. Y. Tao,[73] M. Tat,[70] J. X. Teng,[72,58] V. Thoren,[76] W. H. Tian,[59] Y. Tian,[31,64] Z. F. Tian,[77] I. Uman,[62b] Y. Wan,[55] S. J. Wang,[50]

B. Wang,[1] Bo Wang,[72,58] C. Wang,[19] D. Y. Wang,[46,h] H. J. Wang,[38,k,l] J. J. Wang,[77] J. P. Wang,[50] K. Wang,[1,58] L. L. Wang,[1] L. W. Wang,[34] M. Wang,[50] N. Y. Wang,[64] S. Wang,[38,k,l] S. Wang,[12,g] T. Wang,[12,g] T. J. Wang,[43] W. Wang,[59] W. Wang,[73] W. P. Wang,[35,58,72,o] X. Wang,[46,h] X. F. Wang,[38,k,l] X. J. Wang,[39] X. L. Wang,[12,g] X. N. Wang,[1] Y. Wang,[61] Y. D. Wang,[45] Y. F. Wang,[1,58,64] Y. H. Wang,[38,k,l] Y. L. Wang,[19] Y. N. Wang,[45] Y. Q. Wang,[1] Yaqian Wang,[17] Yi Wang,[61] Z. Wang,[1,58] Z. L. Wang,[73] Z. Y. Wang,[1,64] D. H. Wei,[14] F. Weidner,[69] S. P. Wen,[1] Y. R. Wen,[39] U. Wiedner,[3] G. Wilkinson,[70] M. Wolke,[76] L. Wollenberg,[3] C. Wu,[39] J. F. Wu,[1,8] L. H. Wu,[1] L. J. Wu,[1,64] Lianjie Wu,[19] X. Wu,[12,g] X. H. Wu,[34] Y. H. Wu,[55] Y. J. Wu,[31] Z. Wu,[1,58] L. Xia,[72,58] X. M. Xian,[39] B. H. Xiang,[1,64] T. Xiang,[46,h] D. Xiao,[38,k,l] G. Y. Xiao,[42] H. Xiao,[73] Y. L. Xiao,[12,g] Z. J. Xiao,[41] C. Xie,[42] X. H. Xie,[46,h] Y. Xie,[50] Y. G. Xie,[1,58] Y. H. Xie,[6] Z. P. Xie,[72,58] T. Y. Xing,[1,64] C. F. Xu,[1,64] C. J. Xu,[59] G. F. Xu,[1] M. Xu,[72,58] Q. J. Xu,[16] Q. N. Xu,[30] W. L. Xu,[67] X. P. Xu,[55] Y. Xu,[40] Y. C. Xu,[78] Z. S. Xu,[64] F. Yan,[12,g] L. Yan,[12,g] W. B. Yan,[72,58] W. C. Yan,[81] W. P. Yan,[19] X. Q. Yan,[1,64] H. J. Yang,[51,f] H. L. Yang,[34] H. X. Yang,[1] J. H. Yang,[42] R. J. Yang,[19] T. Yang,[1] Y. Yang,[12,g] Y. F. Yang,[43] Y. X. Yang,[1,64] Y. Z. Yang,[19] Z. W. Yang,[38,k,l] Z. P. Yao,[50] M. Ye,[1,58] M. H. Ye,[8] Junhao Yin,[43] Z. Y. You,[59] B. X. Yu,[1,58,64] C. X. Yu,[43] G. Yu,[13] J. S. Yu,[25,i] M. C. Yu,[40] T. Yu,[73] X. D. Yu,[46,h] C. Z. Yuan,[1,64] J. Yuan,[34] J. Yuan,[45] L. Yuan,[2] S. C. Yuan,[1,64] Y. Yuan,[1,64] Z. Y. Yuan,[59] C. X. Yue,[39] Ying Yue,[19] A. A. Zafar,[74] F. R. Zeng,[50] S. H. Zeng,[63] X. Zeng,[12,g] Y. Zeng,[25,i] Y. J. Zeng,[59] Y. J. Zeng,[1,64] X. Y. Zhai,[34] Y. C. Zhai,[50] Y. H. Zhan,[59] A. Q. Zhang,[1,64] B. L. Zhang,[1,64] B. X. Zhang,[1] D. H. Zhang,[43] G. Y. Zhang,[19] H. Zhang,[72,58] H. Zhang,[81] H. C. Zhang,[1,58,64] H. H. Zhang,[59] H. Q. Zhang,[1,58,64] H. R. Zhang,[72,58] H. Y. Zhang,[1,58] J. Zhang,[59] J. Zhang,[81] J. J. Zhang,[52] J. L. Zhang,[20] J. Q. Zhang,[41] J. S. Zhang,[12,g] J. W. Zhang,[1,58,64] J. X. Zhang,[38,k,l] J. Y. Zhang,[1] J. Z. Zhang,[1,64] Jianyu Zhang,[64] L. M. Zhang,[61] Lei Zhang,[42] P. Zhang,[1,64] Q. Zhang,[19] Q. Y. Zhang,[34] R. Y. Zhang,[38,k,l] S. H. Zhang,[1,64] Shulei Zhang,[25,i] X. M. Zhang,[1] X. Y. Zhang,[40] X. Y. Zhang,[50] Y. Zhang,[1] Y. Zhang,[73] Y. T. Zhang,[81] Y. H. Zhang,[1,58] Y. M. Zhang,[39] Yan Zhang,[72,58] Z. D. Zhang,[1] Z. H. Zhang,[1] Z. L. Zhang,[34] Z. X. Zhang,[19] Z. Y. Zhang,[43] Z. Y. Zhang,[77] Z. Z. Zhang,[45] Zh. Zh. Zhang,[19] G. Zhao,[1] J. Y. Zhao,[1,64] J. Z. Zhao,[1,58] L. Zhao,[1] Lei Zhao,[72,58] M. G. Zhao,[43] N. Zhao,[79] R. P. Zhao,[64] S. J. Zhao,[81] Y. B. Zhao,[1,58] Y. X. Zhao,[31,64] Z. G. Zhao,[72,58] A. Zhemchugov,[36,b] B. Zheng,[73] B. M. Zheng,[34] J. P. Zheng,[1,58] W. J. Zheng,[1,64] X. R. Zheng,[19] Y. H. Zheng,[64] B. Zhong,[41] X. Zhong,[59] H. Zhou,[35,50,o] J. Y. Zhou,[34] S. Zhou,[6] X. Zhou,[77] X. K. Zhou,[6] X. R. Zhou,[72,58] X. Y. Zhou,[39] Y. Z. Zhou,[12,g] Z. C. Zhou,[20] A. N. Zhu,[64] J. Zhu,[43] K. Zhu,[1] K. J. Zhu,[1,58,64] K. S. Zhu,[12,g] L. Zhu,[34] L. X. Zhu,[64] S. H. Zhu,[71] T. J. Zhu,[12,g] W. D. Zhu,[41] W. J. Zhu,[1] W. Z. Zhu,[19] Y. C. Zhu,[72,58] Z. A. Zhu,[1,64] J. H. Zou,[1] and J. Zu[72,58]

(BESIII Collaboration)

[1]*Institute of High Energy Physics, Beijing 100049, People's Republic of China*
[2]*Beihang University, Beijing 100191, People's Republic of China*
[3]*Bochum Ruhr-University, D-44780 Bochum, Germany*
[4]*Budker Institute of Nuclear Physics SB RAS (BINP), Novosibirsk 630090, Russia*
[5]*Carnegie Mellon University, Pittsburgh, Pennsylvania 15213, USA*
[6]*Central China Normal University, Wuhan 430079, People's Republic of China*
[7]*Central South University, Changsha 410083, People's Republic of China*
[8]*China Center of Advanced Science and Technology, Beijing 100190, People's Republic of China*
[9]*China University of Geosciences, Wuhan 430074, People's Republic of China*
[10]*Chung-Ang University, Seoul, 06974, Republic of Korea*
[11]*COMSATS University Islamabad, Lahore Campus, Defence Road, Off Raiwind Road, 54000 Lahore, Pakistan*
[12]*Fudan University, Shanghai 200433, People's Republic of China*
[13]*GSI Helmholtzcentre for Heavy Ion Research GmbH, D-64291 Darmstadt, Germany*
[14]*Guangxi Normal University, Guilin 541004, People's Republic of China*
[15]*Guangxi University, Nanning 530004, People's Republic of China*
[16]*Hangzhou Normal University, Hangzhou 310036, People's Republic of China*
[17]*Hebei University, Baoding 071002, People's Republic of China*
[18]*Helmholtz Institute Mainz, Staudinger Weg 18, D-55099 Mainz, Germany*
[19]*Henan Normal University, Xinxiang 453007, People's Republic of China*
[20]*Henan University, Kaifeng 475004, People's Republic of China*
[21]*Henan University of Science and Technology, Luoyang 471003, People's Republic of China*
[22]*Henan University of Technology, Zhengzhou 450001, People's Republic of China*
[23]*Huangshan College, Huangshan 245000, People's Republic of China*
[24]*Hunan Normal University, Changsha 410081, People's Republic of China*

[25]Hunan University, Changsha 410082, People's Republic of China
[26]Indian Institute of Technology Madras, Chennai 600036, India
[27]Indiana University, Bloomington, Indiana 47405, USA
[28a]INFN Laboratori Nazionali di Frascati, I-00044, Frascati, Italy
[28b]INFN Sezione di Perugia, I-06100, Perugia, Italy
[28c]University of Perugia, I-06100, Perugia, Italy
[29a]INFN Sezione di Ferrara, I-44122, Ferrara, Italy
[29b]University of Ferrara, I-44122, Ferrara, Italy
[30]Inner Mongolia University, Hohhot 010021, People's Republic of China
[31]Institute of Modern Physics, Lanzhou 730000, People's Republic of China
[32]Institute of Physics and Technology, Peace Avenue 54B, Ulaanbaatar 13330, Mongolia
[33]Instituto de Alta Investigación, Universidad de Tarapacá, Casilla 7D, Arica 1000000, Chile
[34]Jilin University, Changchun 130012, People's Republic of China
[35]Johannes Gutenberg University of Mainz, Johann-Joachim-Becher-Weg 45, D-55099 Mainz, Germany
[36]Joint Institute for Nuclear Research, 141980 Dubna, Moscow region, Russia
[37]Justus-Liebig-Universitaet Giessen, II. Physikalisches Institut, Heinrich-Buff-Ring 16, D-35392 Giessen, Germany
[38]Lanzhou University, Lanzhou 730000, People's Republic of China
[39]Liaoning Normal University, Dalian 116029, People's Republic of China
[40]Liaoning University, Shenyang 110036, People's Republic of China
[41]Nanjing Normal University, Nanjing 210023, People's Republic of China
[42]Nanjing University, Nanjing 210093, People's Republic of China
[43]Nankai University, Tianjin 300071, People's Republic of China
[44]National Centre for Nuclear Research, Warsaw 02-093, Poland
[45]North China Electric Power University, Beijing 102206, People's Republic of China
[46]Peking University, Beijing 100871, People's Republic of China
[47]Qufu Normal University, Qufu 273165, People's Republic of China
[48]Renmin University of China, Beijing 100872, People's Republic of China
[49]Shandong Normal University, Jinan 250014, People's Republic of China
[50]Shandong University, Jinan 250100, People's Republic of China
[51]Shanghai Jiao Tong University, Shanghai 200240, People's Republic of China
[52]Shanxi Normal University, Linfen 041004, People's Republic of China
[53]Shanxi University, Taiyuan 030006, People's Republic of China
[54]Sichuan University, Chengdu 610064, People's Republic of China
[55]Soochow University, Suzhou 215006, People's Republic of China
[56]South China Normal University, Guangzhou 510006, People's Republic of China
[57]Southeast University, Nanjing 211100, People's Republic of China
[58]State Key Laboratory of Particle Detection and Electronics, Beijing 100049, Hefei 230026, People's Republic of China
[59]Sun Yat-Sen University, Guangzhou 510275, People's Republic of China
[60]Suranaree University of Technology, University Avenue 111, Nakhon Ratchasima 30000, Thailand
[61]Tsinghua University, Beijing 100084, People's Republic of China
[62a]Istinye University, 34010, Istanbul, Turkey
[62b]Near East University, Nicosia, North Cyprus, 99138, Mersin 10, Turkey
[63]University of Bristol, H H Wills Physics Laboratory, Tyndall Avenue, Bristol, BS8 1TL, United Kingdom
[64]University of Chinese Academy of Sciences, Beijing 100049, People's Republic of China
[65]University of Groningen, NL-9747 AA Groningen, The Netherlands
[66]University of Hawaii, Honolulu, Hawaii 96822, USA
[67]University of Jinan, Jinan 250022, People's Republic of China
[68]University of Manchester, Oxford Road, Manchester, M13 9PL, United Kingdom
[69]University of Muenster, Wilhelm-Klemm-Strasse 9, 48149 Muenster, Germany
[70]University of Oxford, Keble Road, Oxford OX13RH, United Kingdom
[71]University of Science and Technology Liaoning, Anshan 114051, People's Republic of China
[72]University of Science and Technology of China, Hefei 230026, People's Republic of China
[73]University of South China, Hengyang 421001, People's Republic of China
[74]University of the Punjab, Lahore-54590, Pakistan
[75a]University of Turin, I-10125, Turin, Italy
[75b]University of Eastern Piedmont, I-15121, Alessandria, Italy
[75c]INFN, I-10125, Turin, Italy
[76]Uppsala University, Box 516, SE-75120 Uppsala, Sweden

[77]*Wuhan University, Wuhan 430072, People's Republic of China*
[78]*Yantai University, Yantai 264005, People's Republic of China*
[79]*Yunnan University, Kunming 650500, People's Republic of China*
[80]*Zhejiang University, Hangzhou 310027, People's Republic of China*
[81]*Zhengzhou University, Zhengzhou 450001, People's Republic of China*

[a]Deceased.
[b]Also at the Moscow Institute of Physics and Technology, Moscow 141700, Russia.
[c]Also at the Novosibirsk State University, Novosibirsk, 630090, Russia.
[d]Also at the NRC "Kurchatov Institute", PNPI, 188300, Gatchina, Russia.
[e]Also at Goethe University Frankfurt, 60323 Frankfurt am Main, Germany.
[f]Also at Key Laboratory for Particle Physics, Astrophysics and Cosmology, Ministry of Education; Shanghai Key Laboratory for Particle Physics and Cosmology; Institute of Nuclear and Particle Physics, Shanghai 200240, People's Republic of China.
[g]Also at Key Laboratory of Nuclear Physics and Ion-beam Application (MOE) and Institute of Modern Physics, Fudan University, Shanghai 200443, People's Republic of China.
[h]Also at State Key Laboratory of Nuclear Physics and Technology, Peking University, Beijing 100871, People's Republic of China.
[i]Also at School of Physics and Electronics, Hunan University, Changsha 410082, China.
[j]Also at Guangdong Provincial Key Laboratory of Nuclear Science, Institute of Quantum Matter, South China Normal University, Guangzhou 510006, China.
[k]Also at MOE Frontiers Science Center for Rare Isotopes, Lanzhou University, Lanzhou 730000, People's Republic of China.
[l]Also at Lanzhou Center for Theoretical Physics, Lanzhou University, Lanzhou 730000, People's Republic of China.
[m]Also at the Department of Mathematical Sciences, IBA, Karachi 75270, Pakistan.
[n]Also at Ecole Polytechnique Federale de Lausanne (EPFL), CH-1015 Lausanne, Switzerland.
[o]Also at Helmholtz Institute Mainz, Staudinger Weg 18, D-55099 Mainz, Germany.